Photoinduced Electron Transfer at the Core/Shell Interface of Polystyrene−Anthracene−Poly(methacrylic acid) Diblock Copolymer Micelles in Aqueous Media

A. R. Eckert,[†] T. J. Martin,[‡] and S. E. Webber*

Department of Chemistry and Biochemistry and Center for Polymer Research, The University of Texas at Austin, Austin, Texas 78712

Received: September 19, 1996; In Final Form: December 4, 1996[⊗]

We have characterized the photophysics and excited-state electron transfer reactions of polymer micelles formed from diblock polystyrene−(anthracene)-*block*-poly(methacrylic acid). In these studies (anthracene) comprises either a single 1-(2-anthryl)-1-phenylethylene (An) or an average of two vinyl-9,10-diphenylanthracene (vDPA). This architecture is expected to place the chromophores in the interfacial region between the polystyrene core and poly(methacrylic acid) corona. Quenching of the anthryl fluorescence by Tl^+ and two viologens (SPV, 4,4′-bipyridyl-1,1′-bis(propanesulfonate), and MV^{2+}, methyl viologen) demonstrated that access to these chromophores was limited at all pHs, and the rate of diffusion of the viologens was relatively slow. Similar conclusions were drawn from quenching of the ^{3}An* state and the anion radical $SPV^{\bullet-}$ by O_2. We believe this illustrates that the interfacial region of the micelle is not fully deprotonated even at pH 9. It was observed that the fraction of ^{3}An* that was quenched by SPV was smaller than ^{1}An*. This demonstrates the existence of a heterogeneous distribution of anthryl sites such that some ^{3}An* cannot be quenched, which is not the case for ^{1}An*. We conclude that the spatial requirements for quenching these two excited states are not equivalent. Electron transfer quenching by SPV produces $SPV^{\bullet-}$ that is very long-lived, but some unknown reaction removes the anthryl cation radical. As a consequence, we can build up a concentration of $SPV^{\bullet-}$ under steady-state photolysis. The quantum yield of charge separation per quenching event is similar to previous cases we have studied, *ca.* 0.5, but unlike linear polyacids, there is very little pH dependence. This is consistent with the idea that there is minimal deprotonation near the core−corona interface of the micelle.

Introduction

Photoinduced electron transfer[1,2] continues to be an active area of research motivated by the desire to create efficient artificial photosynthetic systems.[3] The fundamental measure of merit for such systems is a high quantum yield for creation of charge-separated ion pairs, a long lifetime for these pairs such that useful chemistry can intercept the ion-pair recombination process, and long-term stability of the various components of the system (*e.g.*, a large turnover number for the photon to ion-pair process).

Morishima has reviewed the incorporation of photoactive polycyclic aromatic hydrocarbons into the backbone of polyelectrolytes.[4] Morishima's review article emphasizes polyelectrolyte systems in which the fluorescence quencher is an aqueous phase viologen, which also serves as the electron acceptor. "Hydrophobic compartmentalization" of the chromophore reduces the rate of fluorescence quenching (the forward electron transfer) but increases the yield of charge-separated ions.[5] "Static quenching" typically reduces the charge separation yield, but Morishima also noted some exceptions to this general rule. These findings lead to questions that have been addressed by Mataga[6] and others[7] on how "tight" or "loose" the initial ion pair is at the time of the quenching event and what effect the solvent cage or environment has in helping to separate the geminate ion pair.

We and others have been involved in the study of photoinduced charge separation between viologens and polyelectrolyte bound aromatic chromophores, particularly poly(methacrylic acid), PMA, with anthracene chromophores.[8−11] This earlier work reports a consistent increase in charge-separated yield with a decrease in pH which is ascribed to increased "hydrophobic protection" (which is equivalent to the term "compartmentalization", discussed above). Hsiao and Webber[12] also demonstrated this effect by preferential adsorption of chromophores covalently attached to PMA onto water-soluble polystyrene latex particles. These latex systems produced exceptional yields of ion pairs with radical anion lifetimes in the millisecond range.

The work reported here utilizes a very different kind of hydrophobic polystyrene−aqueous interface using polymer micelles comprised of diblock polystyrene−poly(methacrylic acid), PS−PMA. The block copolymers were labeled with anthracene moieties at the junction point by anionic polymerization techniques (see Chart 1 for structure and abbreviations).[13] It is expected that the chromophores reside near or at the micelle interface in an environment that is similar to the compartmentalization produced by the collapsed PMA polyelectrolyte at low pH.

A high singlet state charge separation yield is obtained for PS−vDPA−PMA using SPV (4,4′-bipyridyl-1,1′-bis(propanesulfonate)) as a quencher, and the lifetime of the $SPV^{\bullet-}$ anion is exceptionally long. In fact, it is possible to build up a steady-state concentration of $SPV^{\bullet-}$ with photolysis at 370 nm. However, it is also found that the anthracene cation radical vanishes on the nanosecond time scale. It seems that some part of the system is acting as a sacrificial reagent with respect to the cation radical. The anthracene moiety is not destroyed for

[†] Present address: IBM Microelectronics, 1580 Route 52, MS 40E, Hopewell Junction, NY 12533.

[‡] Present address: CONDEA Vista Company, 12024 Vista Parke Drive, Austin, TX 78726-4026.

[⊗] Abstract published in *Advance ACS Abstracts,* February 1, 1997.

S1089-5639(96)02891-5 CCC: $14.00

CHART 1

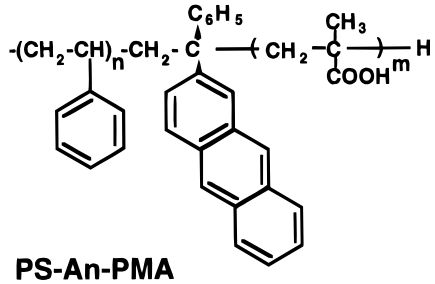

PS-An-PMA

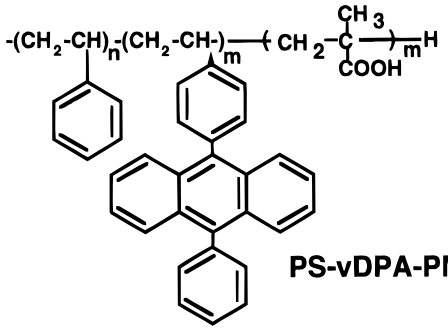

PS-vDPA-PMA

TABLE 1: Molecular Weight Data for the Block Copolymers

polymer	PS block	total[a]
PS−An−PtBMA[b]	29 500	53 000
PS−vDPA−PtBMA[c]	36 000	71 000

[a] Molecular weight is in g/mol and was measured by GPC before hydrolysis of *tert*-butyl groups. [b] Reference 13. [c] Reference 14.

each charge separation event, although the turnover number for the DPA chromophore is not high (estimated to be *ca.* 17).

The Results section of this paper is divided into two major parts: (1) a section describing the photophysics of these systems and (2) a section concerning charge separation properties.

Experimental Section

A. Materials. Synthesis of the block copolymers was achieved by the technique of anionic polymerization and has been described elsewhere.[13,14] The PS−An−PMA polymer was initiated with the potassium complex of 1-(1-methoxy-1-methylethyl)naphthalene to which styrene monomer was added and allowed to react to completion. Then 1-(2-anthryl)-1-phenylethylene was added to attach only one anthracene group at the junction before the *tert*-butylmethacrylate monomer was added. Hydrolysis of the *tert*-butyl groups with hydrochloric acid at ∼ 100 °C results in the final product of PS−An−PMA as verified by NMR spectroscopy. The PS−vDPA−PMA block copolymer was synthesized using cumyl potassium in the initiation of styrene. Addition of vinyldiphenylanthracene (vDPA) followed by *tert*-butyl methacrylate and hydrolysis produced a similar block copolymer, except that an average of 1.8 vDPA groups were added to the junction point. The molecular weight data for both polymers before hydrolysis are presented in Table 1.

Micelles were prepared by dissolving block copolymers in dioxane at a concentration of 4 mg/mL and then slowly adding water. Dialysis is started at 80% dioxane/20% water and proceeds in 10% increments of aqueous 0.1 M $NaNO_3$ until 100% aqueous solution is achieved. Stock solutions of micelles were further dialyzed in the appropriate buffer solutions prepared from pHydrion Chemvelopes of powdered buffer salts. Dissolving the diblock copolymer directly in 80/20 dioxane water did not produce small monodisperse micelles, but instead the polymer precipitated upon dialysis. This physical behavior is different than our other studies of PS−PMA micelles,[15] even though the length of the PS and PMA blocks are typical of the polymers used in the earlier studies. We speculate that the additional hydrophobic character imparted by the anthracene moieties at the interface may be the reason for this. In general, the preparation of aqueous solutions of polymer micelles is highly dependent on the polymer. For pH < 4 PS−PMA micelles tend to aggregate over time, with the addition of ions or while carrying out simple operations like filtration, *etc*.

Synthesis of SPV (4,4′-bipyridyl-1,1′-bis(propanesulfonate) was accomplished as follows: a fluorescent impurity was removed from 4,4′-bipyridyl from using a silica gel column with acetone as the eluting solvent. The purified 4,4′-bipyridyl was then dissolved in methanol, and a 5 times molar excess of 1,3-propane sultone was added.[9] The solvent was then removed under vacuum at *ca.* 40 °C to produce SPV. The solid was washed with acetone and was dissolved in water and precipitated twice with acetone. The solid was redissolved in water, filtered, and precipitated with spectral grade methanol. The product was collected by filtration and vacuum-dried. NMR and mass spectrometry gave satisfactory analysis. Methyl viologen was obtained from Sigma Chemical Co. and was used as received. All other chemicals were obtained from Aldrich.

B. Quasi-Elastic Light Scattering, QELS. Hydrodynamic diameters were measured by quasi-elastic light scattering on a Brookhaven 2030 AT system, as has been described in detail earlier.[16]

C. Fluorescence Spectroscopy. Steady-state fluorescence spectra were measured with a Spex Fluorolog fluorimeter equipped with double monochromators for both the excitation and emission radiation. Data collection uses a personal computer with the SPEX DM3000 software.

Time-resolved fluorescence decays were measured using the method of time correlated single photon counting. The measurement system at the Center for Fast Kinetics Research (CFKR) has been described in detail earlier.[17] Excitation was at 350 nm, from a pyridine 1 dye laser pumped by a Coherent Antares Nd:YAG. Emission was monitored at $\lambda \sim 400$ nm for PS−An−PMA and $\lambda \sim 420$ nm for PS−vDPA−PMA micelles using a Hamamatsu R1564U microchannel plate photomultiplier tube with a monochromator. The instrument response of the system is *ca.* 70 ps. The decay of fluorescence intensity is conveniently fit by a multiexponential function:

$$I(t) = \sum_i \alpha_i \exp(-t/\tau_i) \quad (1)$$

Components as short as 50 ps can be detected using deconvolution methods, given adequate signal to noise. The average lifetimes quoted later were calculated using the lifetimes and preexponential factors calculated for the deconvoluted decay with the following formula:

$$\langle \tau \rangle = \sum_i \alpha_i \tau_i / \sum_i \alpha_i \quad (2)$$

D. Transient Absorption Spectroscopy. Laser flash photolysis measurements were also carried out at the Center for Fast Kinetics Research.[8,18,19] The pump source was a Q-switched Quantel YG 481 Nd:YAG laser operated at the third harmonic (355 nm, ∼30 mJ/pulse, 11 ns pulse width). The probe source was a high-pressure 150 W xenon arc lamp which was pulsed for 1 ms periods to produce a bright and stable interrogation source. The time-dependent optical density of $SPV^{\bullet -}$ was monitored at 400 and 600 nm with the concentration

being measured at the latter wavelength based on an extinction coefficient of 1.37×10^4 M^{-1} cm^{-1}, as in our earlier work.[18,20] Decay curves were analyzed according to first-order kinetics. No photoionization of the chromophores was observed at the laser power used for this work.

The charge separation quantum yields were estimated as follows: the concentration of $SPV^{\bullet-}$ anion was obtained by extrapolating the time-dependent optical density to the time at which the laser pulse was fired. The yield of $SPV^{\bullet-}$ anion per excited state, $\phi_{SPV\bullet-}$, is calculated by dividing the SPV anion concentration by the concentration of excited-state species,[12]

$$\phi_{SPV^{\bullet-}} = [SPV^{\bullet-}]/[D^*] \quad (3)$$

in which D* corresponds to ^{1,3}An* or ^{1}DPA* (DPA undergoes negligible intersystem crossing). The concentration of excited states, [D*], is determined from the method of relative actinometry using the zinc tetrakis(sulfonatophenyl)porphyrin (ZnTPPS) triplet state as a standard.[23] The extinction coefficient for the triplet state of ZnTPPS is 55 200 M^{-1} cm^{-1} at 460 nm with a quantum yield of 0.84. Solutions of ZnTPPS were prepared with the same OD as the micelle. The concentration of excited states was about 15% of the total concentration for both micelles. For this work the micelle concentrations were kept constant at *ca.* 1 mg/mL such that there is no difference between the extent of light scattering for the two micelle systems. The optical density was ~0.04 for PS−An−PMA at $\lambda = 355$ nm and ~0.10 for PS−vDPA−PMA. This reflects the difference in extinction coefficients of the two chromophores and the fact that there are ~2 vDPA chromophores per chain rather than just one, as is the case for PS−An−PMA.

The quantum yield of charge separation per quenching event, ϕ_{cs}, is calculated by dividing the yield of anions by the fraction of chromophores quenched at a specific SPV concentration (I and I_0 are the fluorescence intensities with and without quencher):

$$\phi_{cs} = \phi_{SPV^{\bullet-}}/[1 - I/I_0] \quad (4)$$

In the limit of 100% quenching we calculate a charge separation yield (ϕ_{cs}^{∞}) from the intercept of a double-reciprocal plot of inverse yield, $(\phi_{SPV\bullet-})^{-1}$, vs inverse quencher concentration.[19]

E. Picosecond Excitation Experiments. Picosecond absorption measurements as a function of time after the exciting pulse (355 nm) were carried out at The Center for Fast Kinetics Research. The interrogation continuum pulse traverses a variable distance delay line before striking the sample, and this system has been described in detail elsewhere.[22]

Results

A. Characterization of the Hydrodynamic Diameter of Micelles as a Function of pH. Poly(methacrylic acid), PMA, is a weak acid polyelectrolyte whose degree of deprotonation with pH is known to vary in a complex manner.[23−26] Chain stretching at high pH is evident in aqueous phase micelles when the shell is PMA,[27] as is most easily demonstrated by the measurement of the hydrodynamic diameter, d_h (Figure 1). In these experiments stock solutions of micelles in 0.1 M $NaNO_3$ were diluted into solutions of buffers from pH 4 to pH 11. The maximum chain extension appears to be reached by pH 7 and above, where the polyacid is significantly deprotonated.[28] As we will discuss later, the degree of deprotonation is not expected to be uniform within the corona, and in fact the region near the PS−PMA interface may not be deprotonated to any appreciable extent. The slight decrease of d_h at pH 11 is a result of the increased ionic strength. Below pH 4 the shell is extensively protonated, and precipitation or aggregation of micelles is much more likely to occur and was often observed. We also note that the An block copolymers have a lower molecular weight but formed micelles of larger diameter than their vDPA counterparts.[29] A small amount of polystyrene homopolymer was detected in the An sample, but it is unclear what effect this may have on the aggregation number of the micelles. One may speculate that the hydrophobicity of the two chromophores may have some influence on the aggregation number of the micelle.

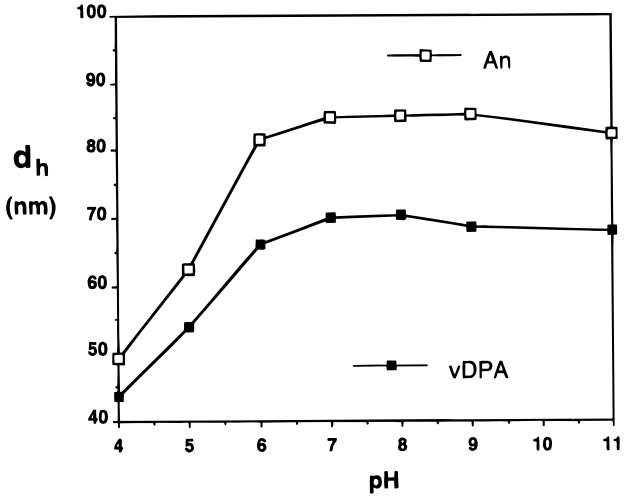

Figure 1. Hydrodynamic diameter of micelles as a function of pH.

B. Photophysical Characterization: Quenching Studies. We have probed the chromophore environment at the micelle core/shell interface as a function of pH with three different fluorescence quenchers Tl^+, SPV, and MV^{2+}. Each provides slightly different information about the interface. They all display the expected trend of a decreasing quenching rate with lower pH. This pH effect has been the basis for the term "hydrophobic protection" or "compartmentalization", as has been discussed earlier. However, in these micelles the effect of pH is orders of magnitude smaller than in linear polyacids and provides indirect evidence for the low degree of deprotonation near the PS−PMA interface. The magnitude of the quenching of the singlet state plays an essential role in our calculation of charge separation efficiency (see eq 4).

The steady-state quenching data often require a nonlinear Stern−Volmer equation:

$$I_0/I = 1 + A[Q] + B[Q]^2 + ... \quad (5)$$

in which I_0 and I have the same meaning as in eq 4. In classical Stern−Volmer kinetics $B = 0$ and $A = K_{SV} = k_q\tau_0$, the product of the second-order quenching constant k_q and the normal excited-state lifetime.

A 1−2 nm red shift in the emission spectra for micelles at pH 9 compared to pH 5 provides spectroscopic evidence that shell protonation does affect the chromophore environment. This indicates that the chromophores are in a less polar environment at lower pH.[26,30]

Fluorescence Quenching with Tl^+. We and others have used the Tl^+ ion to study the exposure to water of a chromophore covalently bound to a polyelectrolyte or in other amphiphilic environments.[31,32] The idea is that this simple ion will not penetrate into hydrophobic regions, unlike the more complex viologens, which have "surfactant" character (see the next subsection). Quenching with $TlNO_3$ produced significant negative curvature in the Stern−Volmer plot indicating that the chromophores are protected from the aqueous phase (Figure 2).

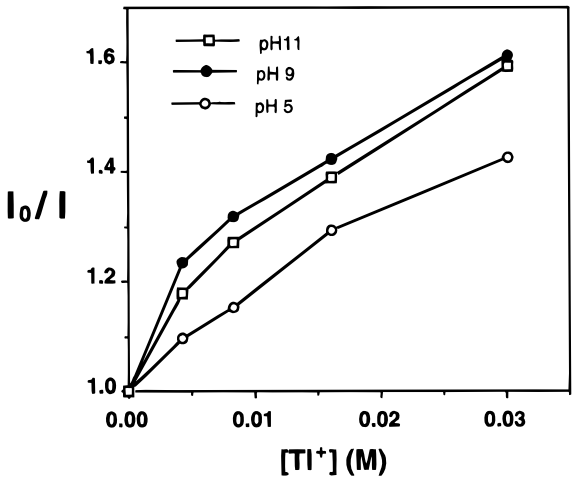

Figure 2. Stern−Volmer plot of fluorescence quenching of vDPA micelles by Tl^+ at pH 5, 9, and 11.

TABLE 2: Tl^+ Fluorescence Quenching Parameters for vDPA Micelles as a Function of pH[a]

pH	f_a	K_a	k_q ($\times 10^{-10}$) M^{-1} s^{-1} [b]
5	0.47	53	0.82
9	0.41	201	3.1
11	0.44	119	1.8
average	0.44		
PSS^-Na^+−vDPA[c]	1.0		140[c]

[a] See eq 6 of text. [b] $k_q = K_a/\tau_0$. [c] For poly(styrene sulfonate)-*co*-vDPA (see ref 32).

We obtain a satisfactory fit to the quenching data with a two-state model:[33]

$$I_0/(I_0 - I) = 1/f_a + 1/K_a f_a[Q] \quad (6)$$

In this equation f_a is the fraction of chromophores accessible to the quencher, and K_a is the Stern−Volmer constant for the accessible fraction. From our data fit we calculate an average value of $f_a \sim 0.44$ and a pH-dependent K_a (Table 2). We ascribe the drop in K_a from pH 9 to pH 11 to ionic strength effects. (This accuracy of this quantity is not high, *ca.* ±15%.) The f_a values are independent of pH within experimental error. In an attempt to "anneal" the micelle core, we studied the fluorescence quenching of these micelles after being exposed to benzene, which is known to swell the micelle core.[15c,e] This would be expected to relieve inhomogeneities that are "frozen in" during micelle preparation. No change in Tl^+ quenching was observed.[34]

The most important aspect of this quenching data is that there is such a small effect of pH. For the corresponding linear polyacid at high pH k_q has been measured as *ca.* 1×10^{12} M^{-1} s^{-1} for low ionic strength and *ca.* 1×10^{11} M^{-1} s^{-1} for high ionic strength.[32] For pH ≈ 3, k_q of 4.3×10^7 M^{-1} s^{-1} for pyrene-tagged methacrylic acid was obtained.[31] This reduced pH sensitivity is one piece of evidence that suggests that deprotonation in the interfacial region is greatly reduced compared to the corresponding linear PMA. This is reasonable based on the lower "effective dielectric constant" expected in this region and has also been suggested by various theoretical studies.[35−37] As far as we know, this is the first experimental evidence for this phenomenon.

Fluorescence Quenching with SPV. In Figure 3 we present Stern−Volmer plots for both micelles at pH 5 and 9, and Table 3 contains the Stern−Volmer constants (see eq 5) for a larger range of pH. The quenching ratio at high pH is much smaller than observed for linear PMA.[8,26] At high pH the Stern−Volmer constant can be fit to a linear equation while at low pH a significant amount of upward curvature requires a second-order polynomial fit to the data. This latter behavior is typically associated with a static quenching mechanism, which suggests SPV−chromophore associations. As in the preceding subsection, the slight decrease from pH 9 to pH 11 is ascribed to the increased ionic strength.[31,32]

SPV is zwitterionic and is inherently a type of surfactant with interfacial activity and is expected to have a much higher affinity for the (PS core)/(aqueous PMA shell) interface compared to the Tl^+ cation. Quenching with SPV has been observed to occur by a long-range electron transfer mechanism,[38] whereas Tl^+ is a collisional quencher. Because of the different expressions

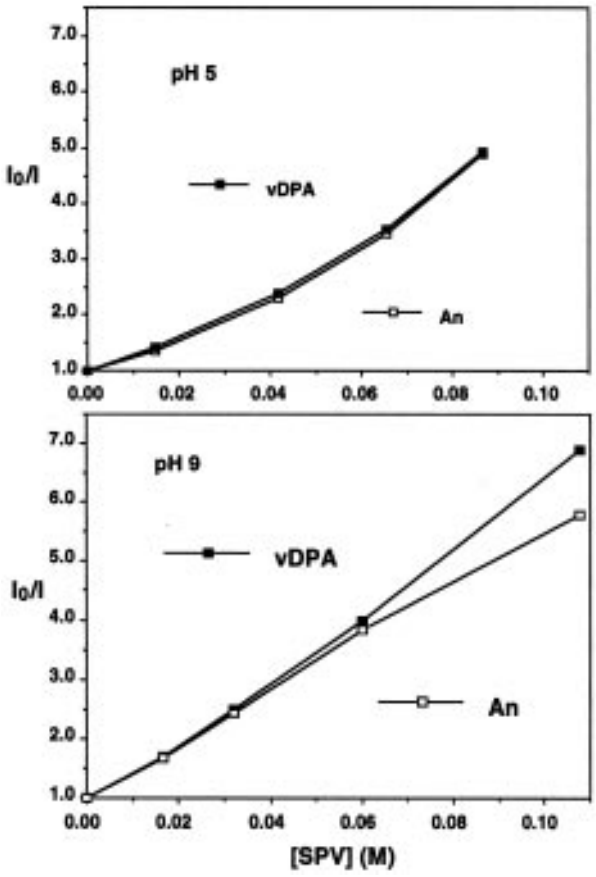

Figure 3. Stern−Volmer plot of fluorescence quenching by SPV of aqueous PS−vDPA−PMA and PS−An−PMA micelles at pH 5 and 9.

TABLE 3: Steady-State Fluorescence Quenching Parameters of Diblock Micelles (PS−An−PMA, PS−vDPA−PMA) and Linear Polymers (PMA−An, PMA−vDPA) with SPV at Various pHs[a]

	PS-An-PMA			PS−vDPA−PMA		
pH	*A*	*B*	$[Q]_{1/2}$[b]	*A*	*B*	$[Q]_{1/2}$[b]
4	16	100	48	18	140	42
5	18	310	35	22	270	32
6	11.5	53	67	13.4	63	59
9	45		22	53		19
11	30.5		33	33		30

	PMA−An[c]			PMA−vDPA[c]		
pH	*A*	*B*	$[Q]_{1/2}$	*A*	*B*	$[Q]_{1/2}$
2.8	52	360	17	20	300	33
11	230	4.6×10^4	2.8	96	1.9×10^3	8.9

[a] For pH's 4, 5 eq 5 was used. For pH 9 and 11 a linear Stern−Volmer fit produced an adequate fit. [b] For ease of comparison of systems with different quenching functions, $[Q]_{1/2}$ represents the concentration of quencher (in mM) required for $I_0/I = 2$. [c] From ref. 8.

TABLE 4: Fluorescence Quenching Parameters for Micelles and Linear Polyelectrolyte with MV^{2+} as a Function of pH

(a) Data for Micelles

	PS−An−PMA		PS−vDPA−PMA	
pH	K_{SV} (M^{-1})[a]	$[Q]_{1/2}$ (mM)[b]	K_{SV} (M^{-1})[a]	$[Q]_{1/2}$ (mM)[b]
4	174	5.7	307	3.3
5	271	3.7	373	2.7
6	291	3.4	571	1.8
7			1148	0.87
8	995	1.0	1177	0.85
9	1161	0.86	1562	0.64
11	1166	0.86	1567	0.64

(b) Linear PMA−Anthracene System

	PMA−An[c]			PMA−vDPA[c]		
pH	A	B	$[Q]_{1/2}$ (mM)	A	B	$[Q]_{1/2}$ (mM)
2.8	140	1600	6.6	35	300	24
11	8.6×10^3	1.6×10^8	0.057	5.5×10^3	2.3×10^7	0.12

[a] This constant is equivalent to A in eq 4; a satisfactory fit was obtained for $B = 0$. [b] $[Q]_{1/2}$ like Table 3 and is equal to K_{SV}^{-1}. [c] From ref 8.

used to fit the quenching data at different pHs, we also include $[Q]_{1/2}$ in Table 3, the quencher concentration required for $I_0/I = 2$. As can be seen, there is a slight drop in $[Q]_{1/2}$ for pH 5. We cannot offer a persuasive explanation for this observation. We presume that it reflects a "loosening" of the PMA near the interface at pH 5. The $[Q]_{1/2}$ values at pH 9 and 11 are much higher compared to a linear polymer (see Table 3). We believe this further illustrates the relatively small degree of deprotonation near the interface.

Fluorescence Quenching with MV^{2+}. Enhanced quenching efficiency with increasing pH is observed using methyl viologen, MV^{2+}. A linear fit to the Stern−Volmer plots for both micelles at all pH values is satisfactory (data not shown). We note that the K_{SV} values at pH 9 and 11 are very similar (see Table 4a), unlike the slight difference observed for SPV (Table 3). The increase in K_{SV} for pH higher than 8 implies that even though the shell is fully expanded by pH 7 according to the d_h values (Figure 1), a higher fraction of the carboxylic acid groups in the interfacial region may be deprotonated. As the pH is lowered, the K_{SV} values decrease, which could reflect both slower diffusion due to the more viscous environment of the collapsing PMA shell and diminished electrostatic attraction for MV^{2+}. Note that the $[Q]_{1/2}$ values (just the inverse of K_{SV}) are much smaller than for SPV, which reflects the high quenching efficiency of MV^{2+}. We believe that this is primarily due to its smaller size and net +2 charge. We do not believe that this is an energetic effect since the reduction potential for SPV is −0.65 V[20] and for MV^{2+} it is −0.68 V,[39] both vs SCE.[40] We note that quenching of the vDPA micelles is slightly more efficient than the An micelles.

The comparison to linear polymers in Table 4b is interesting. The quenching of linear PMA−anthracene at pH 2.8 is less efficient (vDPA) or approximately equally efficient (An) as for the micelles at pH 4 (which is approximately the lower limit of pH for stable solutions; see the Experimental Section). At pH 11 the quenching is *ca.* 5−10 times less efficient for the micelle than the linear polymer. These factors are similar to SPV, despite the much higher overall quenching efficiency for MV^{2+}.

When we attempted to use MV^{2+} for electron transfer experiments below pH 7 (see later), we observed aggregation and precipitation of the micelles during the transient absorption measurements. A side reaction is possible between H^+ and MV^0 (formed by the disproportionation reaction between $MV^{\bullet+}$ species) to form polymeric products.[41] It is reasonable that the long lifetime and high local concentration of $MV^{\bullet+}$ might encourage this reaction. In any case, this effect prevented accurate measurement of the charge separation yield with MV^{2+} as the electron acceptor, although yields are qualitatively similar to SPV. The aggregation was not as prevalent in fluorescence quenching measurements due to the lower concentrations of quencher used and the much smaller photon flux.

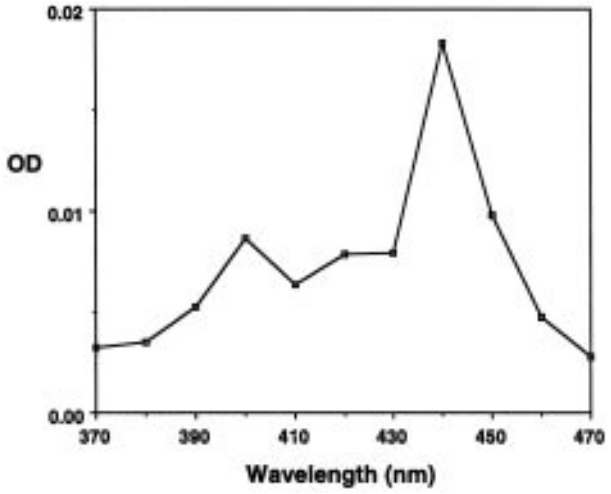

Figure 4. Transient absorption spectra of the An triplet state at a ~1 μs delay after the laser pulse at pH 5.

TABLE 5: Survival of the An Triplet State as a Function of SPV Concentration and Oxygen Quenching at pHs 5 and 9

		pH 5			pH 9		
curve[a]	SPV (mM)	OD[b]	$f_s(^3An^*)$[c]	$f_s(^1An^*)$[d]	OD[b]	$f_s(^3An^*)$[c]	$f_s(^1An^*)$[d]
1	0	30.5	1.00	1.00	18.5	1.00	1
2	10.2	27.0	0.89	0.82	18.5	1.00	0.69
3	29.2	25.0	0.82	0.56	13.5	0.73	0.43
4	62.4	21.0	0.69	0.30	11.0	0.59	0.26
5	62.4 + O_2	15.5	0.51		6.5	0.35	

[a] Refers to curve numbers in Figure 5. [b] The optical density at 440 nm immediately after the laser pulse in units of mAU. [c] $f_s(^3An^*)$ is the fraction of surviving triplet states observed compared to curve 1. $f_s(^3An^*) = OD_x/OD_1$ where x signifies the curve number in Figure 5. [d] $f_s(^1An^*)$ is the fraction of surviving singlet states, given by I/I_0 at a given quencher concentration.

SPV Quenching of the Anthracene Triplet State in PS−An−PMA Micelles. Past work has demonstrated an enhancement of the charge separation yield from $^3An^*$ due to the spin-forbidden recombination of the ion pair.[17] Therefore, we have characterized the effect of pH on the quenching of the An triplet state by SPV. (Recall that the vDPA micelles do not produce a measurable triplet population.) Because of our interest in excited-state electron transfer, we do not study Tl^+ and MV^{2+}, the latter being excluded because of the difficulties mentioned above. Also, MV^{2+} can be directly excited at 355 nm light when complexed with PMA.[41] It is known from earlier work that the An triplet-state lifetime and yield is affected by the environment when adsorbed onto latex particles.[17,18] The observed $^3An^*$ spectral shape is normal (see Figure 4) and independent of pH. The triplet yield and lifetime are very sensitive to changes in pH (see Tables 5 and 6). Figure 5 demonstrates the very different effects of adding SPV to solutions of An micelles at pH 5 and 9. At pH 5 (Figure 5a) we observe only modest decay of the $^3An^*$ over a 450 μs time scale with increasing concentration of SPV, although there is a significant decrease in initial OD. At pH 9 (Figure 5b) the triplet yield is lower. (Compare the OD values immediately after the laser pulse.) Upon the first addition of SPV at pH 9 we observe no change in the initial concentration of $^3An^*$, but there is a decrease in the triplet lifetime. Upon further addition of SPV

TABLE 6: Average Lifetime Parameters for the An Triplet State

		pH 5					pH 9				
curve[a]	SPV (mM)	α_1	τ_1	α_2	τ_2	$\langle^3\tau_{avg}\rangle^b$	α_1	τ_1	α_2	τ_2	$\langle^3\tau_{avg}\rangle^b$
1	0	0.05	0.20	0.95	10.8	10.2	0.37	0.15	0.63	3.08	2.0
2	10.2	0.07	0.14	0.93	4.9	4.6	0.45	0.07	0.55	2.3	1.3
3	29.2	0.09	0.16	0.91	7.2	6.6	0.44	0.06	0.56	2.7	1.5
4	62.4	0.11	0.12	0.89	4.4	3.9	0.45	0.04	0.55	1.5	0.834
5	62.4 + O_2	1.0				0.0068[c]	1.0				0.0022[c]

[a] Refers to curve numbers in Figure 5. Note that the data was fit out to a maximum time of 1 ms because of the inherent instability of the interrogation lamp. Therefore, the long lifetime (τ_2) will not be very accurate although good accuracy is expected for α_2. [b] $\langle^3\tau_{avg}\rangle = \sum_i\alpha_i\tau_i/\sum_i\alpha_i$; all lifetimes in ms. [c] Fit to a single exponential.

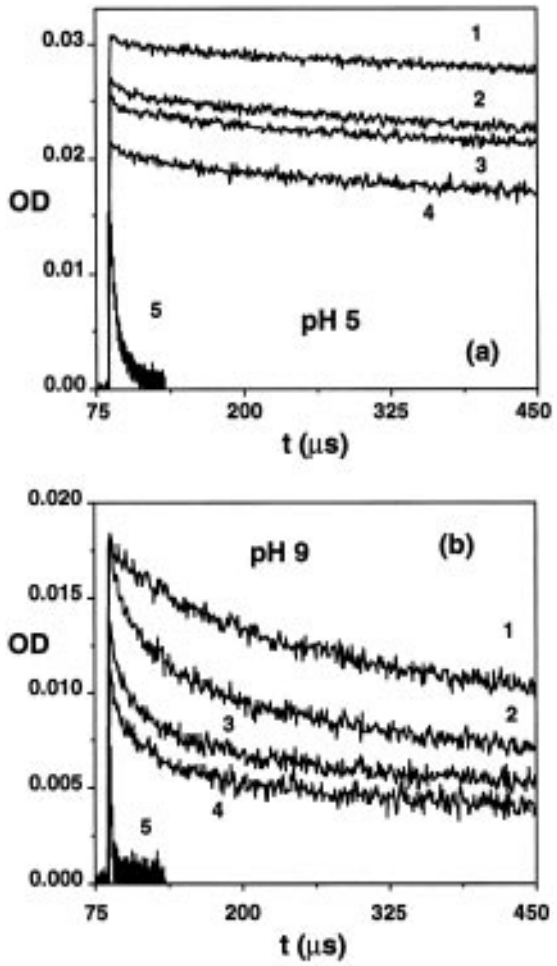

Figure 5. (a) Time-dependent optical density of the ^{3}An* for pH 5 micelles as a function of SPV concentration with N_2 deaeration, 1−4, and with O_2, 5 (λ_{obs} = 440 nm). See Table 5 for SPV concentrations. (b) Like (a) except pH 9.

we observe a lowering of the initial OD and faster decay. For pH 9 the decays are biexponential, which may be a result of a distribution of chromophore environments. In Table 5 we quantify the change in the initial OD for the An triplet as a function of added quencher concentration. Because the yield of the An triplet state is based on the survival of the singlet state, we must take into account the fraction of ^{1}An* that survive. ($f_s(^1\text{An}^*)$) equals I/I_0 at a given quencher concentration.) We can compare this value with the fraction of ^{3}An* that is present 1 μs after the laser pulse, relative to the unquenched sample. We observe that the fraction of triplets that survive is higher than singlets. Since the loss of the triplet is less than the loss of its precursor singlet state, we conclude that there is enhanced intersystem crossing for the chromophores that are more "compartmentalized" by the micelle core, which in turn have a higher probability of escaping quenching by SPV. There is no evidence for hindered access to ^{1}An* from fluorescence quenching, so it seems that the spatial separation requirement for quenching of ^{1}An* and ^{3}An* by SPV is different.

Adding oxygen after the last addition of SPV further reduces the initial OD of ^{3}An*, and it is the fastest decay trace in Figure 5a,b (curve 5). The triplet lifetime is reduced by *ca.* 2 orders of magnitude, and the quenching is 3 times more efficient for pH 9 than pH 5 (see Table 6). This is consistent with the idea that an expanded shell permits better access to the interfacial region. The pseudo-first-order quenching rates ($k(O_2)$) for the An triplet state may be estimated to be 1.5×10^5 and 4.5×10^5 s^{-1} for pH 5 and 9, respectively. Using Henry's law of partial pressures for O_2 in H_2O, we calculate an oxygen concentration of $[O_2] = 2.5 \times 10^{-4}$ M.[42] A bimolecular rate constant, $k_{q(O2)}$, can estimated from the average pseudo-first-order rate constants

$$k_{q(O2)} = k(O_2)/[O_2] \tag{7}$$

from which we obtain 0.60×10^9 and 1.8×10^9 M^{-1} s^{-1} for pH 5 and 9. These rates of quenching are on the same order of magnitude as the O_2 quenching of the SPV anion (see later). We also note that these rates are lower than diffusion controlled for an aqueous solution[43] (7.0×10^9 M^{-1} s^{-1}).

C. Photoinduced Electron Transfer to SPV. The standard kinetic scheme we use to analyze our electron transfer process is given by eqs 8−12. Photoinduced electron transfer at the micelle interface as a function of pH can be characterized by the charge separation yield (eq 11) and the decay kinetics of the ion radical species produced (eq 10):

$$\text{D} + h\nu \rightarrow {}^{2S+1}\text{D}^* \tag{8}$$

$${}^{2S+1}\text{D}^* \xrightarrow[k_0]{} \text{D} + \text{heat and/or emission} \tag{9a}$$

$${}^{2S+1}\text{D}^* + \text{A} \xrightarrow[k_q]{} {}^{2S+1}[\text{D}^{\bullet+},\text{A}^{\bullet-}] \tag{9b}$$

$${}^{2S+1}[\text{D}^{\bullet+},\text{A}^{\bullet-}] \xrightarrow[k_{cs}]{} \text{D}^{\bullet+} + \text{A}^{\bullet-} \tag{10a}$$

$${}^{2S+1}[\text{D}^{\bullet+},\text{A}^{\bullet-}] \xrightarrow[k_b]{} \text{D} + \text{A} + \text{heat} \tag{10b}$$

The quantum yield of charge separation is given by

$$\phi_{cs} = \frac{k_{cs}}{k_{cs} + k_b} \tag{11}$$

The fraction of excited states quenched in (9b) is given by

$$f_q = \frac{k_q[\text{A}]}{k_0 + k_q[\text{A}]} \tag{12}$$

Step 9b is the excited-state quenching/forward electron transfer which forms a geminate ion pair. This ion pair can undergo a fast (pico- or femtosecond) recombination to the

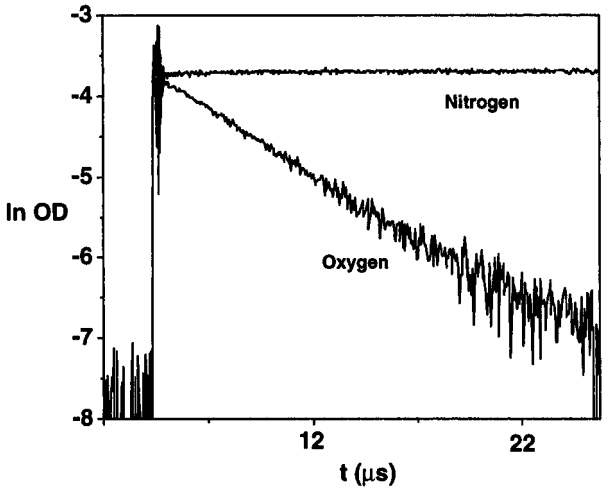

Figure 6. Time-dependent optical density of the $SPV^{\bullet-}$ anion (at 600 nm) from the PS−vDPA−nPMA micelles at pH 5 with nitrogen deaeration and in the presence of O_2 (air saturated).

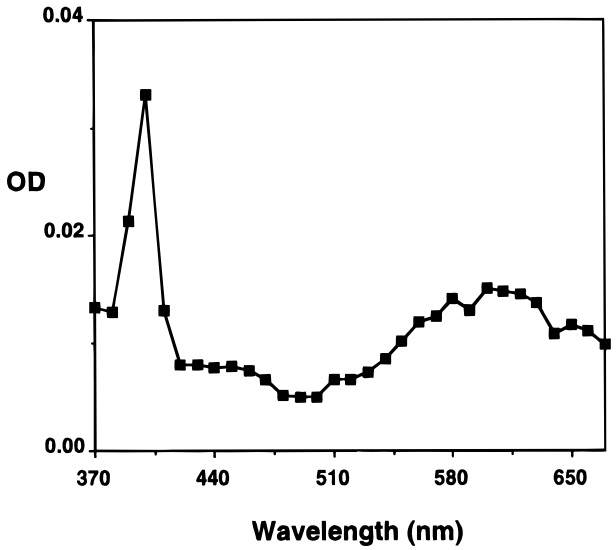

Figure 7. Transient absorption spectra of the $SPV^{\bullet-}$ anion produced from fluorescence quenching of PS−vDPA−PMA micelles at a ∼1 μs delay after the laser pulse.

ground-state species (step 10b) or become a charge-separated ion pair (step 10a) with yield ϕ_{cs}. This charge-separated ion pair can then undergo back electron transfer to the ground state at the diffusion-limited rate of decay of the ion pairs or participate in other redox reactions.

We carried out three different types of transient absorption experiments designed to characterize the production of the SPV anion: (1) laser excitation and transient absorption spectroscopy on a nano- to millisecond time scale; (2) steady-state irradiation and detection of the SPV anion using a diode array UV−vis spectrophotometer that allows observation on a time scale in excess of seconds; (3) picosecond absorption spectroscopy in order to observe the initial electron transfer event. We only present the spectral results for PS−vDPA−PMA, but reaction yields and rates are given for both micelles. The order of our discussion follows the order in which experiments were carried out, as we sought to characterize the long lifetime of the $SPV^{\bullet-}$ anion radical and the absence of the $DPA^{\bullet+}$ cation radical.

Microsecond Transient Absorption Spectroscopy. Figure 6 compares the time-dependent optical density for SPV in solutions that were either deaerated with N_2 or O_2 saturated, over a 25 μs time scale using the Q-switched laser system described in the Experimental Section (∼10 ns laser pulse at 355 nm). For the former case at all pH values there is no observable decay of the $SPV^{\bullet-}$ out to the millisecond time scale with either polymer micelle. Observation at longer times is difficult because of interrogation lamp instabilities. We will discuss the rate of reaction between O_2 and $SPV^{\bullet-}$ in a later section.

The electrostatic repulsion between the negatively charged SPV anion and the polyelectrolyte is known to retard the diffusive back-reaction (the reverse of step 10a).[44] Additionally, long lifetimes for the ion pair are encouraged by "compartmentalization" at the hydrophobic micelle interface. A typical SPV radical anion absorption spectra is displayed in Figure 7. The SPV anion has prominent peaks at 400 and 600 nm with the OD at the latter wavelength being used for our calculations of quantum yield. We attempted to observe the vDPA cation by carrying out the quenching in the presence of O_2 since $SPV^{\bullet-}$ preferentially reacts with O_2. The $DPA^{\bullet+}$ absorption spectra is known to have an extinction coefficient of ∼8900 M^{-1} cm^{-1} at 600 nm,[8,45] with relatively distinctive peaks. The $SPV^{\bullet-}$ absorption is completely removed by oxygen, but only base line noise is observed (spectrum not shown). Similarly, no vDPA cation was found in preliminary experiments with MV^{2+}, although experiments using this quencher were not pursued for the reasons discussed earlier. We suspect that the cation species is rapidly reduced, but the mechanism of the reduction reaction is unknown. It is possible that the $DPA^{\bullet+}$ spectrum is greatly distorted by the micelle interfacial environment, but the picosecond experiments (see later) favor the former explanation.

TABLE 7: Quantum Yields of Charge Separation with PS−An−PMA Diblock Copolymer Micelles as a Function of pH

pH	[SPV] (mM)	$1 - I/I_0$	$\phi_{SPV^{\bullet-}}$ [a]	ϕ_{cs} [b]	(ϕ_{cs}^{∞}) [b]
4	30.7	0.37	0.46	1.24[c]	
	46.1	0.49	0.47	0.96	
	76.8	0.65	0.53	0.83	(0.67)
5	30.5	0.46	0.41	0.90	
	45.7	0.60	0.43	0.72	
	76.2	0.76	0.47	0.61	(0.51)
6	48.7	0.41	0.49	1.20[c]	
	81.2	0.56	0.60	1.07[c]	
	130.0	0.71	0.57	0.81	(0.72)
9	24.0	0.52	0.27	0.52	
	42.0	0.65	0.26	0.40	
	72.0	0.76	0.28	0.37	(0.32)
11	51.2	0.58	0.29	0.50	
	89.6	0.70	0.26	0.37	
	154.0	0.81	0.32	0.40	(0.34)

[a] $\phi_{SPV^{\bullet-}}$ was calculated with eq 3. [b] ϕ_{cs} was calculated according to eq 4, and ϕ_{cs}^{∞} was calculated from the intercept of a double-reciprocal plot of $(\phi_{cs})^{-1}$ vs $[SPV]^{-1}$.[19] [c] $\phi_{cs} > 1$ is nonphysical but illustrates that the experimental uncertainty in ϕ_{cs} is significant because it combines several OD measurements (see eq 3 and the discussion immediately following).

Tables 7 and 8 present the charge separation efficiencies for An and vDPA micelles as a function of pH (see eq 11). For the PS−An−PMA micelles at low pH the limiting quantum yield of charge separation, ϕ_{cs}^{∞}, is 0.5−0.7 and drops to 0.3 at higher pH. For the vDPA micelles no systematic pH effect was apparent, and the ϕ_{cs}^{∞} values are usually smaller. The relatively small pH effect for both micelles is also consistent with our previous contention that the pH does not significantly effect the polarity and/or charge density around the chromophore. Recall that only a slight red shift (1−2 nm) was observed in the emission spectra as a function of pH whereas when chromophores are solvated in media of different polarity the spectral shift is typically larger.[30]

TABLE 8: Quantum Yields of Charge Separation with PS−vDPA−PMA Diblock Copolymer Micelles as a Function of pH

pH	[SPV] (mM)	$1 - I/I_0$	$\phi_{SPV\bullet-}$ [a]	ϕ_{cs}	(ϕ_{cs}^{∞}) [b]
4	46.1	0.53	0.22	0.42	
	80.7	0.70	0.18	0.26	
	115.3	0.80	0.23	0.28	(0.21)
5	30.5	0.48	0.33	0.68	
	45.7	0.61	0.38	0.61	
	76.2	0.76	0.40	0.52	(0.46)
6	48.7	0.45	0.42	0.95	
	85.2	0.62	0.42	0.68	
	122.0	0.72	0.47	0.65	(0.53)
9	24.0	0.56	0.21	0.38	
	42.0	0.69	0.18	0.26	
	72.0	0.79	0.21	0.26	(0.21)
11	51.2	0.58	0.26	0.44	
	89.6	0.71	0.26	0.37	
	153.6	0.81	0.28	0.34	(0.31)

[a] $\phi_{SPV\bullet-}$ was calculated with eq 3. [b] ϕ_{cs} was calculated according to eq 4, and ϕ_{cs}^{∞} was calculated from the intercept of a double-reciprocal plot of $(\phi_{cs})^{-1}$ vs $[SPV]^{-1}$.[19]

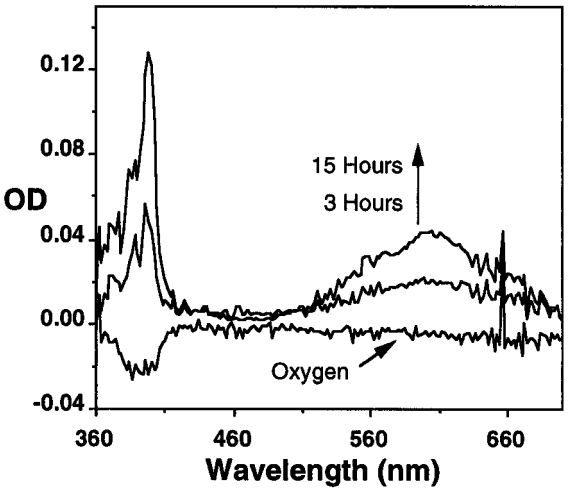

Figure 8. UV−vis difference absorption spectra (relative to zero irradiation) of PS−vDPA−PMA micelles and sufficient SPV to quench 0.8 of the singlet, at 3 and 15 h of irradiation at 370 nm, followed by the introduction of oxygen.

Steady-State Production of the SPV Anion. In these experiments we studied only PS−vDPA−PMA micelles to avoid any contribution from the triplet. Constant irradiation was carried out at 370 nm using the double-excitation monochromator of our SPEX fluorimeter. The photon flux was 1.85×10^{14} photons s^{-1} as measured by chemical actinometry using Aberchrome 540.[46] For a nitrogen-deaerated solution of pH 9 vDPA micelles and SPV sealed in a gas-tight cell, this resulted in a measurable buildup of the SPV anion. Figure 8 is the difference UV−vis absorption spectra of a pH 9 solution after 3 and 15 h of irradiation and the initial unirradiated spectrum. Upon the addition of oxygen, we observe the expected disappearance of the SPV anion and a ∼10% decrease in the region that corresponds to absorption by vDPA. There is no $vDPA^{\bullet+}$ absorption observed in the 600−750 nm region.[8,45] Thus, we conclude that the long-time survival of the SPV anion is the result of some adventitious "sacrificial reagent" that removes the vDPA cation.

It was found that after the initial 3 h exposure the SPV anion would disappear within an hour. But upon further exposure the SPV anion remained stable for longer periods of time. This effect could be due to residual oxygen reacting with the SPV anion. We estimate the 1/e lifetime as *ca.* 40 min over the full period of the photolysis. A rough calculation of ϕ_{cs} is possible from these results. The steady-state concentration of $SPV^{\bullet-}$ is *ca.* 2×10^{-6} M. Given a flux of 1.85×10^{14} photons/s into the cuvette, with approximately one-third absorbed (OD = 0.15 at 370 nm), the fraction of DPA singlets quenched (*ca.* 0.8) and a $SPV^{\bullet-}$ lifetime of *ca.* 40 min, we obtain $\phi_{cs} \approx 1.5$, which is nonphysical but, given the errors in the above estimate, is in order of magnitude agreement with our value of 0.3 in Table 8. The yield of $SPV^{\bullet-}$ per incident photon, averaged over the full 15 h exposure, is much lower, *ca.* 5×10^{-3}. Of course, if the $SPV^{\bullet-}$ could be intercepted to do useful chemical work at a rate much faster than its lifetime, then the yield of "useful product" per incident photon would be given by the product $\phi_{cs}(1 - I/I_0) \approx 0.24$. It must be stressed that these yields include the reaction in which the $DPA^{\bullet+}$ is reduced by some unknown component of the system, which we assume is associated with the micelle (see later discussion).

Despite the fact that $DPA^{\bullet+}$ is not observed, some loss of DPA does occur under long-term photolysis in the presence of SPV. There is no loss of DPA in the absence of SPV under identical photolysis conditions. The quantum yield of the loss of DPA per 370 nm photon absorbed is estimated to be *ca.* 0.05, which if corrected for the fraction that is quenched increases to *ca.* 0.06, or a turnover number of *ca.* 17. We do not know what reaction(s) are responsible for this small value, but this illustrates a fundamental problem with organic molecules as photon energy transducers, *i.e.*, lack of long-term photochemical stability.

At pH 5 we were not able to build up a measurable concentration of the SPV anion although no appreciable decay in the transient absorption out to 10 ms was observed, similar to pH 9. In the next subsection we estimate that the lifetime of $SPV^{\bullet-}$ at pH 5 is less than 200 ms. A reaction analogous to that referred to earlier between H^+ and MV^0 may contribute to the loss of the SPV anion at pH 5.[41,47] However, we do not observe significant loss of SPV during photolysis, based on the relatively small change in the fluorescence intensity.

We note that after a week in storage at pH 9 with exposure to ambient light that micelle samples became yellow, and the absorption at ∼400 nm increases dramatically. Thin layer chromatography confirms this is a small molecule and not part of the micelle, which we presume to be some product from the SPV.

Picosecond Transient Absorption Experiments for PS−vDPA−PMA. At pH 5 and 9 the SPV anion is observed at minimum delay between the pump and probe pulse (Figure 9, only pH 9 data is shown). If we delay the probe pulse by 3.2 ns, no decay of the SPV anion is observed, as expected from our other observations. We conclude that electron transfer occurs between donors and acceptors that are in proximity rather than by a diffusional quenching process. In our steady-state fluorescence quenching Stern−Volmer plots with SPV the upward curvature is consistent with the idea of contact quenching at the core−shell interface. With oxygen aeration the optical density of the SPV is also a maximum at zero time delay for both pH 5 and 9. The transient spectrum of the O_2-saturated sample shows a smaller overall optical density (by a factor of *ca.* 5), due in part to singlet-state quenching by O_2. The relative intensity in the 500−800 nm region is now approximately equal to the 380−400 nm region. This is consistent with the presence of $DPA^{\bullet+}$ on this time scale and suggests that the reaction that removes this species is on the >10 ns time scale.

For pH 9 micelles with N_2 deaeration we observed a buildup of the SPV anion with each consecutive pulse at 5 Hz. This is

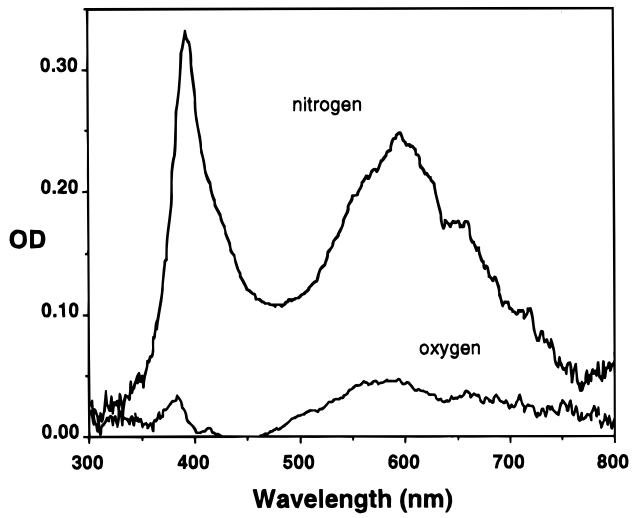

Figure 9. Spectra of pH 9 vDPA micelles with SPV anion production using a picosecond excitation pulse, with and without O_2 present (λ = 355 nm, [SPV] = 0.081 M, fraction of fluorescence quenched 0.77).

TABLE 9: Pseudo-First-Order Rate Constants for Oxygen Quenching of the SPV Anion in An and vDPA Micelles

pH	$k_{(O_2)}$ An ($\times 10^{-5}$) (s^{-1})	$k_{(O_2)}$ vDPA ($\times 10^{-5}$) (s^{-1})	% [$SPV^{\bullet -}$] at 1 μs
4	1.53	3.30	95
5	0.89	1.63	96
6	2.46	3.21	85
9	1.46	2.62	78
11	1.95	2.46	55
	av 1.66 ± 0.59	av 2.64 ± 0.67	

expected, given the extremely long lifetime of the SPV anion. This buildup was not observed at pH 5, which implies that the lifetime at pH 5 must be less than the inverse of the pulse frequency, 200 ms. In our microsecond experiments we measured a lifetime in excess of 10 ms. Evidently, there is a big difference in the SPV anion lifetime at pH 5 and 9. One contribution to this effect could be that the polyelectrolyte shell at pH 9 is negatively charged and will repel the SPV anion, thereby reducing the probability for back-reaction at the interface.[20] The loss of $DPA^{\bullet +}$ might be favored if the acid group is deprotonated (*e.g.*, the photo Kolbe reaction), although we did not observe the anthryl cation at any pH.

Oxygen Quenching of the SPV Anion. Oxygen is known to remove the electron from the $SPV^{\bullet -}$ anion by the reaction

$$SPV^{\bullet -} + O_2 \rightarrow SPV + O_2^{\bullet -} \qquad (13)$$

while the donor radical cations remain unaffected.[9] We discuss the rate of O_2 quenching (in air-saturated solution) of $SPV^{\bullet -}$ by way of comparison to the ^{3}An* quenching studies discussed earlier.

The time-dependent optical density of the $SPV^{\bullet -}$ anion decays exponentially when oxygen replaces nitrogen (see Figure 6). The pseudo-first-order rate constants, $k(O_2)$, at different pH are listed in Table 9 with an average of 2.64×10^5 for the vDPA micelles and 1.66×10^5 for the An micelles. There seems to be no systematic change of $k(O_2)$ with pH, except for the decrease at pH 5, similar to the SPV fluorescence quenching (Table 3, *cf.* $[Q]_{1/2}$ values given there). Although the standard deviation is large (25% for both micelles at similar pH values), the An micelles always have the smaller rate constants. Using the same estimate of $[O_2]$ as for the triplet-state quenching, we calculate average $k(O_2)$ values of 0.67×10^9 and 1.1×10^9 M^{-1} s^{-1} for PS−An−PMA and PS−vDPA−PMA micelles, respectively. These values are similar to triplet state quenching

SCHEME 1

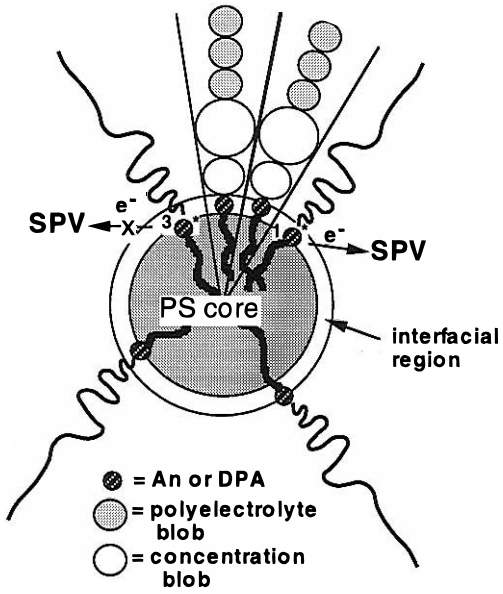

and are an order of magnitude lower than the diffusion-limited reaction rate in water. A discussed earlier, a quantitative comparison of these bimolecular rates is not justified because the local concentration of O_2 in the core, interfacial region, and bulk water can be significantly different. The fact that the rate constants are slightly smaller for the An micelles may be a result of their larger size, which slows the diffusion of the $SPV^{\bullet -}$ anion from the micelle interface into the outer corona where it can be readily quenched by O_2.

A large percentage of $SPV^{\bullet -}$ anion observable at the earliest time (*ca.* 1 μs) with nitrogen deaeration persists in the presence of oxygen. The percent of unquenched $SPV^{\bullet -}$ (in Table 9) for each pH is the average for both micelle types because the values for the two micelles are similar to each other. At low pH the micelles are more effective in protecting the SPV anion from static quenching by O_2 than at high pH. This suggests that as the shell deprotonates the interfacial region where $SPV^{\bullet -}$ is produced is more accessible to oxygen, but this could also be an effect of the local solubility of O_2. Note that the quenching of singlet excited state in air-saturated solution is negligible due to the short singlet-state lifetime. (Saturation with pure O_2 is required to produce a significant effect.)

Discussion

Fluorescence quenching of mid-tagged anthracene chromophores in diblock copolymer micelles by Tl^+, MV^{2+}, and SPV is similar to linear PMA−An and PMA−vDPA in homogeneous solution at pH 2.8. At this low pH it is believed that PMA becomes hypercoiled into "microdomains" around the chromophores.[50] Furthermore, the quenching efficiency changes relatively little in going from pH 4 to pH 11. We have mentioned earlier that theory has suggested that deprotonation should be diminished near the surface of a convex "annealed polyelectrolyte brush".[36] This is represented in Scheme 1, based on the representation in ref 37. Near the interfacial region the polyacid is largely protonated, forming increasingly large "concentration blobs" away from the interface (similar to the case of a neutral polymer micelle corona). At a sufficiently large distance from the interface the polyacid is deprotonated, and smaller polyelectrolyte blobs are formed. These latter structures are essentially equivalent to a linear, stretched polyelectrolyte chain. We have not examined the effect of ionic strength, but Lyatskaya *et al.*[36] predict that at high ionic strength the radial dependence of deprotonation is greatly diminished.

We note that at every pH the quenching efficiencies (as measured by $[Q]_{1/2}$) are similar for the two types of micelles, despite the longer lifetime of the An moiety. There are approximately two vDPA groups per polymer chain such that some enhancement in quenching efficiency could arise from inter- and intrachain energy transfer. The position of the chromophore with respect to the interface could be slightly different because of the chemical structure (see Chart 1). It is perhaps more remarkable how similar these two systems are.

The study of the PS−An−PMA anthracene triplet-state quenching as a function of pH reveals a further element of heterogeneity that must exist at the micelle interface. At pH 9, where the shell is known to be expanded, there is some diffusional quenching of ^{3}An* by SPV. At higher SPV concentrations the interface may become saturated with this "surfactant" zwitterionic molecule, and a static quenching mechanism also plays a role. At pH 5 the quenching is entirely static (see Figure 5). This description is consistent with the upward curvature observed in SPV fluorescence quenching at pH 5. The biexponential character of the triplet state decay at pH 9 suggests that the anthracene chromophores are in at least two environments. We speculate that one population may be more exposed to the aqueous phase (presumably the shorter lifetime component observed in Figure 5 and Table 6), and the other population of An moieties is "deeper" in the micelle core. Additional evidence for a mixed population of An chromophores at the micelle interface is provided by the differing fraction of surviving triplet and singlet states as SPV is added (*cf.* $f_s(^3$An*) and $f_s(^1$An*) in Table 5). This implies that either the intersystem crossing yield is different for these environments, or the quenching rate of ^{3}An* is lower than for the ^{1}An* state, or both. The proposed inequality in quenching efficiency for these two excited states and the disorder at the interface are also represented in the cartoon of Scheme 1.

The rates of the oxygen quenching of the triplet state are approximately 3 times larger at pH 9 than pH 5. Unlike SPV quenching, *all* ^{3}An* are quenched by O_2. Past work has found that mid-tagged chromophores of PS−PMA are fairly immobile.[27] Because the rate constants for O_2 quenching of ^{3}An* are similar to the rates observed for the quenching of $SPV^{\bullet-}$, we conclude that the diffusion of $SPV^{\bullet-}$ is very slow in the interfacial region. However, one difficulty with these comparisons is that one expects differential solubility for O_2 for the polystyrene core/shell region of the micelle.

A striking aspect of the diblock micelle systems is the extremely long lifetime of the SPV anion after the charge separation event and the absence of the anthracene cation. Picosecond absorption spectroscopy indicates that the electron transfer is faster than the anthracene singlet state lifetime (*i.e.*, no buildup of $SPV^{\bullet-}$ is observed), and the $SPV^{\bullet-}$ is quenched relatively slowly by O_2. This finding is consistent with our picture of this interface as a highly viscous environment. The difference between the pico- and microsecond transient absorption spectra suggests that $DPA^{\bullet+}$ is present immediately after quenching.

It is plausible that the cation is being rapidly reduced by some species that is present in the interfacial region of the micelle. It is well-known that $DPA^{\bullet+}$ reacts with water, with the stoichiometry illustrated in (14):[49]

$$2DPA^{\bullet+} + 2H_2O \rightarrow DPA + DPA(OH)_2 + 2H^+ \quad (14)$$

In this same study the reaction of $DPA^{\bullet+}$ with a variety of other species, including acetate, was discussed, although without much detail. Thus, a candidate for reduction of the anthracene cation is the reaction with a nearby carboxyl group, *e.g.*, analogous to the photo Kolbe decarboxylation reaction reported by Kraeutler and Bard

$$h^+_{TiO_2} + RCOOH \rightarrow R^{\bullet} + CO_2 + H^+ \quad (15)$$

in which $h^+_{TiO_2}$ is a photogenerated hole in TiO_2.[50] Stramel and Thomas[41] propose an analogous reaction of PMA with photoexcited MV^{2+}, *i.e.*

$$(MV^{2+})^* + -(CH_3)(CO_2^-)C-CH_2^- \rightarrow MV^{\bullet+} + -(CH_2{=}C(CO_2^-) + {}^{\bullet}CH_2- + H^+ \quad (16)$$

Stramel and Thomas note that there is no reaction with simple model acids, so the high local density of carboxylate groups in PMA is essential (*i.e.*, a "polymer effect"). However, Stramel and Thomas find that reaction 16 is ineffective at low pH, which we believe is the situation that exists near the core−corona interface regardless of bulk pH.

A variety of reactions could occur after a reaction like 14 or 15, such as radical coupling to the anthryl moiety or cross-linking between neighboring radicals formed in independent reactions. The former could represent one loss mechanism for anthryl groups, but since we estimate a turnover number on the order of 17, radical coupling cannot accompany each photoredox reaction. If extensive cross-linking or depolymerization in the interfacial region were to occur, then we might expect that the polymer network in the vicinity of the anthracene moiety would be changed, such that the efficiency of fluorescence quenching for a photolyzed sample would be modified. This is not found to be the case. The hydrodynamic diameter primarily reflects the exterior dimension of the corona and therefore is insensitive to processes near the core of the micelle. On the other hand, reactions 14−16 would produce a substantial decrease in pH,[51] which would affect d_h (see Figure 1). No change in d_h is observed upon extensive photolysis in the presence of SPV. One could search for CO_2 in the headspace above the solution, but given the rather high solubility of CO_2 in water,[52] we do not see this as a feasible experiment. Thus, the nature of the "sacrificial reagent" remains unknown.

Summary

The work described herein has characterized the photophysics and photochemistry of two anthracene chromophores at a micelle interface as a function of pH. The polyelectrolyte shell is contracted at pH 4 and expands with increasing pH with maximum extension above pH 7. Fluorescence quenching with Tl^+ has shown that the chromophore is *ca.* 50% accessible to inorganic ions. Quenching with amphiphilic SPV and MV^{2+} species demonstrates 100% accessibility to the excited single-state chromophores. The relatively inefficient singlet and triplet quenching with SPV and the relatively slow reaction of ^{3}An* and $SPV^{\bullet-}$ with O_2 suggests that the interface has a higher density of polymer segments than linear PMA at an equivalent pH. For PS−An−PMA micelles the yield and lifetime of the triplet state were enhanced at low pH, presumably because of a modification in the local polarity. Quenching of the triplet state with SPV was very limited and the biexponential decay of the triplet state of the pH 9 micelles suggests a distribution of environments for An chromophores between two extremes: (1) exposed to the aqueous phase and (2) "hidden" in the micelle core. For SPV quenching of the PS−An−PMA singlet state there was no indication of "inaccessible chromophores" (*cf.* Tl^+ quenching). This suggests different spatial requirements for SPV quenching ^{1}An* and ^{3}An*. On the other hand, O_2 was found to quench 100% of the triplet states, demonstrating its high mobility and solubility in the interior of our diblock copolymer micelles.

The quantum yields of charge separation from singlet-state quenching do not vary systematically with pH. No anthryl cation radical was observed for greater than microsecond time scales, suggesting a fast reduction by some species within the micelle structure, perhaps the polyelectrolyte shell. The $SPV^{\bullet-}$ species has an exceptionally long lifetime in higher pH solution, perhaps because it is expelled from the micelle. Since the anthryl cation is not observed on time scales longer than *ca.* 1 μs, the loss of $SPV^{\bullet-}$ at pH < 9 cannot be from back-reaction with the cation.

There are various modifications of micelles of this type that might alter their photoredox chemistry. For example, one could add PS homopolymer to the diblock copolymers at the start of dialysis, which would increase the size of the micelle core and lower the PMA segment density at the core/shell interface. One could swell the micelle core with a variety of preferentially absorbed organic solvents (*e.g.*, benzene) and look for spectral and/or charge separation changes. We have previously demonstrated that micelles of this type adsorb tenatiously to polystyrene films, such that the study of photoredox processes at polymer interfaces seem plausible.[53] However, identification of the adventitious reductant for $An^{\bullet+}$ and $vDPA^{\bullet+}$ will be a major challenge in future work.

Acknowledgment. Financial support of this research by the Department of Energy Basic Sciences program (DE-FG-03-93ER114337) and the Robert A. Welch Foundation (F-356) is gratefully acknowledged.

References and Notes

(1) Fox, M. A.; Chanon, M. *Photoinduced Electron Transfer*; Elsevier: Amsterdam, 1988.
(2) Kavarnos, G. J. *Fundamentals of Photoinduced Electron Transfer*; VCH Publishers: New York, 1993.
(3) Wasielewski, M. R. *Chem. Rev.* **1992**, *92*, 435.
(4) Morishima, Y. *Adv. Polym. Sci.* **1992**, *104*, 51.
(5) Morishima, Y.; Tominaga, Y.; Kamachi, M.; Okada, T.; Hirata, Y.; Mataga, N. *J. Phys. Chem.* **1991**, *95*, 6027.
(6) Mataga, N.; Asahi, T. *J. Phys. Chem.* **1991**, *95*, 1956.
(7) Niwa, T.; Kikuchi, K.; Matsusita, N.; Hayshi, M.; Katagiri, T.; Takahashi, Y.; Miyashi, T. *J. Phys. Chem.* **1993**, *97*, 11960.
(8) Stramel, R. D.; Webber, S. E.; Rodgers, M. A. J. *J. Phys. Chem.* **1989**, *93*, 1928.
(9) Delaire, J. A.; Sanquer-Barrié, M.; Webber, S. E. *J. Phys. Chem.* **1988**, *92*, 1252.
(10) Delaire, J. A.; Sanquer-Barrié, M. *New J. Chem.* **1992**, *16*, 801.
(11) Shand, M. A.; Rodgers, M. A. J.; Webber, S. E. *Chem. Phys. Lett.* **1991**, *177*, 11.
(12) Hsiao, J.-S.; Webber, S. E. *J. Phys. Chem.* **1993**, *97*, 8289.
(13) For PS−An−PMA see: Martin, T. J.; Webber, S. E. *Macromolecules* **1995**, *28*, 8845.
(14) Martin, T. J. Ph.D. Dissertation, The University of Texas at Austin, May 1996.
(15) Cao, T.; Munk, P.; Ramireddy, C.; Tuzar., Z.; Webber, S. E. *Macromolecules* **1991**, *24*, 6300. (b) Procházka, K.; Kiserow, D.; Ramireddy, C.; Tuzar, Z.; Munk, P., Webber, S. E. *Macromolecules* **1992**, *25*, 454. (c) Kiserow, D.; Procházka, K.; Ramireddy, C.; Tuzar, Z.; Munk, P.; Webber, S. E. *Macromolecules* **1992**, *25*, 461. (d) Ramireddy, C.; Tuzar, Z.; Procházka, K.; Webber, S. E.; Munk, P. *Macromolecules* **1992**, *25*, 2541. (e) Tian, M.; Qin, A.; Ramireddy, C.; Webber, S. E.; Munk, P.; Tuzar, Z.; Procházka, K. *Langmuir* **1993**, *9*, 1741. (f) Kiserow, D.; Chan, J.; Ramireddy, C.; Munk, P.; Webber, S. E. *Macromolecules* **1992**, *25*, 5338.
(16) Eckert, A. R.; Hsiao, J.-S.; Webber, S. E. *J. Phys. Chem.* **1994**, *98*, 12025.
(17) Hsiao, J.-S.; Eckert, A. R.; Webber, S. E. *J. Phys. Chem.* **1994**, *98*, 12032.
(18) Hsiao, J.-S.; Webber, S. E. *J. Phys. Chem.* **1992**, *96*, 2892.
(19) Stramel, R. D.; Webber, S. E.; Rodgers, M. A. J. *J. Phys. Chem.* **1988**, *92*, 6625.
(20) Willner, I.; Yang, J.; Laane, C.; Otvos, J.; Calvin, M. *J. Phys. Chem.* **1981**, *85*, 3277. In this reference an extinction coefficienct of 12 800 M^{-1} cm^{-1} was determined.
(21) Carmichael, I.; Hug, G. L. *J. Phys. Chem. Ref. Data* **1986**, *15*, 1. (b) Kalyanasundaram, K.; Neumann, S.; Pallart, M. *J. Phys. Chem.* **1982**, *86*, 5163.
(22) Atherton, S. J.; Hubig, S. M.; Calla, T. J.; Duncanson, J. A.; Snowden, P. T.; Rodgers, M. A. J. *J. Phys. Chem.* **1987**, *91*, 3137.
(23) Katchalsky, A.; Spitnik, P. *J. Polym. Sci.* **1947**, *2*, 432.
(24) Anufrieva, E. V.; Birshtein, T. M.; Nekrasova, T. N.; Ptitsyn, O. B.; Sheveleva, T. V. *J. Polym. Sci., Part C* **1968**, *16*, 3519.
(25) Chu, D. Y.; Thomas, J. K. In Rabek, J. F. *Photophysics and Photochemistry*; CRC Press: Boca Raton, FL, 1992; Vol. 3, p 49. (b) Mandel, M.; Leyte, J. C.; Stadhouder, M. G. *J. Phys. Chem.* **1967**, *71*, 603. (c) Soutar, I.; Swanson, L. *Macromoleucles* **1994**, *27*, 4304.
(26) Delaire, J. A.; Rodgers, M. A. J.; Webber, S. E. *J. Phys. Chem.* **1984**, *88*, 6219.
(27) Chan, J.; Fox, S.; Kiserow, D.; Ramireddy, C.; Munk, P.; Webber, S. E. *Macromolecules* **1993**, *26*, 7016.
(28) A reviewer has pointed out that at pH 7.6 that the degree of ionization of linear PMA would be approximately 0.8, according to the data of ref 24.
(29) For a discussion of the relation between block molecular weight and micelle properties see: Qin, A.; Tian, M.; Ramireddy, C.; Webber, S. E.; Munk, P. *Macromolecules* **1994**, *27*, 120.
(30) Lakowicz, J. R. *Principles of Fluorescence Spectroscopy*; Plenum Press: New York, 1983; Section 7.2, p 190.
(31) Chu, D.-Y.; Thomas, J. K. *Macromolecules* **1984**, *17*, 2142.
(32) Morrison, M. E.; Dorfman, R. C.; Clendening, W. D.; Kiserow, D. J.; Rossky, P. J.; Webber, S. E. *J. Phys. Chem.* **1994**, *98*, 5534.
(33) Reference 30, pp 279−294.
(34) Morrison, M. Unpublished experiments.
(35) Misra, S.; Mattice, W. L.; Napper, D. H. *Macromolecules* **1994**, *27*, 7090.
(36) Lyatskaya, Y. V.; Leermakers, F. A. M.; Fleer, G. J.; Zhulina, E. B.; Birshtein, T. M. *Macromolecules* **1995**, *28*, 3562.
(37) Shusharina, N. P.; Nyrkova, I. A.; Khokhlov, A. R. *Macromolecules* **1996**, *29*, 3167.
(38) Morishima, Y.; Kobayashi, T.; Furui, T.; Nozkura, S. *Macromolecules* **1987**, *20*, 1707.
(39) Itoh, Y.; Morishima, Y.; Nozakura, S. *Photochem. Photobiol.* **1984**, *39*, 451.
(40) See: Wardman, P. *J. Phys. Chem. Ref. Data* **1989**, *18*, 1637, in which the reduction potential for MV^{2+} and SPV are given as −0.45 and −0.36 V, respectively (vs NHE, V(SCE) = V(NHE) − 0.244 V).
(41) Stramel, R. D.; Thomas, J. K. *J. Chem. Soc, Faraday Trans. 2* **1986**, *82*, 799.
(42) Levine, I. N. *Physical Chemistry*, 3rd ed.; McGraw-Hill: New York 1988; p 252. The O_2 Henry's law constants are 44.1 kbar for H_2O and 1.24 for benzene, at 25 °C.
(43) See ref 42, p 560, for k_{diff}. Since $^3An^*$ is not mobile, this value should be divided by 2. The local solubility of O_2 may be higher than our estimate (*cf.* H_2O and benzene in ref 42), which would diminish the calculated $k_q(O_2)$.
(44) Morishima, Y.; Itoh, Y.; Nozakura, S.; Ohno, T.; Kato, S. *Macromolecules* **1984**, *17*, 2264.
(45) Shida, T. *Electronic Absorption of Radical Ions*; Elsevier: Amsterdam, 1988. The extinction coeficient of $DPV^{\bullet+}$ is not given in this tabulation, only the spectrum.
(46) Aberchromics, Ltd. See: Heller, H. G.; Langer, J. R. *J. Chem. Soc., Perkin Trans. 2* **1981**, 341.
(47) In our earlier work on PMA−vDPA (ref 8) we observed complex kinetics for $SPV^{\bullet-}$ for pH < 5, and we speculated that this may be the result of such a protonation reaction.
(48) For a discussion of the possible effect that a hydrophobic chromophore has on inducing "hypercoiling" see: Morawetz, H. *Macromolecules* **1996**, *29*, 2689.
(49) Sioda, R. E. *J. Phys. Chem.* **1968**, *72*, 2322.
(50) Kraeutler, B.; Bard, A. J. *J. Am. Chem. Soc.* **1978**, *100*, 2239.
(51) Based on the absorption of 1.0×10^{18} photons, one can estimate that if reaction 14−16 occurred for each redox quenching event that the pH would decrease to ca. 4.
(52) The Henry's law constant at 25 °C for CO_2 in water is approximately 1.6 kbar (*Handbook of Chemistry and Physics*, 40th ed.; 1959, pp 1706−7).
(53) Cao, T.; Yin, W.; Armstrong, J. L.; Webber, S. E. *Langmuir* **1994**, *10*, 1841.